


## RESEARCH ARTICLE

# Cognitive loading via mental arithmetic modulates effects of blink-related oscillations on precuneus and ventral attention network regions

Caresa C. Liu<sup>1</sup>  | Sujoy Ghosh Hajra<sup>1</sup> | Xiaowei Song<sup>2</sup> | Sam M. Doesburg<sup>3</sup> | Teresa P. L. Cheung<sup>1,2</sup> | Ryan C. N. D'Arcy<sup>1,2</sup>

<sup>1</sup>School of Engineering Science, Simon Fraser University, Burnaby, British Columbia, Canada

<sup>2</sup>Health Sciences and Innovation, Surrey Memorial Hospital, Fraser Health Authority, British Columbia, Canada

<sup>3</sup>Department of Biomedical Physiology and Kinesiology, Simon Fraser University, Burnaby, British Columbia, Canada

## Correspondence

Ryan C.N. D'Arcy, NeuroTech Lab, Charles Barham Pavilion, Surrey Memorial Hospital, 13750 96 Avenue, Surrey, BC V3V 1Z2, Canada.

Email: rdarcy@sfu.ca

## Funding information

Canadian Institutes for Health Research (CIHR) Frederick Banting and Charles Best Canada Graduate Scholarships Doctoral Awards (CGS-D), Grant/Award Number: GSD-140381; Natural Sciences and Engineering Research Council of Canada, Grant/Award Number: RGPIN-2015-04018; Surrey Hospital Foundation Seed Grant

## Abstract

Blink-related oscillations (BROs) have been linked with environmental monitoring processes associated with blinking, with cortical activations in the bilateral precuneus. Although BROs have been described under resting and passive fixation conditions, little is known about their characteristics under cognitive loading. To address this, we investigated BRO effects during both mental arithmetic (MA) and passive fixation (PF) tasks using magnetoencephalography ( $n = 20$ ), while maintaining the same sensory environment in both tasks. Our results confirmed the presence of BRO effects in both MA and PF tasks, with similar characteristics including blink-related increase in global field power and blink-related activation of the bilateral precuneus. In addition, cognitive loading due to MA also modulated BRO effects by decreasing BRO-induced cortical activations in key brain regions including the bilateral anterior precuneus. Interestingly, blinking during MA—but not PF—activated regions of the ventral attention network (i.e., right supramarginal gyrus and inferior frontal gyrus), suggesting possible recruitment of these areas for blink processing under cognitive loading conditions. Time–frequency analysis revealed a consistent pattern of BRO-related effects in the precuneus in both tasks, but with task-related functional segregation within the anterior and posterior subregions. Based on these findings, we postulate a potential neurocognitive mechanism for blink processing in the precuneus. This study is the first investigation of BRO effects under cognitive loading, and our results provide compelling new evidence for the important cognitive implications of blink-related processing in the human brain.

## KEYWORDS

awareness, blink, blink-related oscillations, environmental monitoring, magnetoencephalography, mental arithmetic, neurocognitive mechanisms, precuneus, ventral attention network

## 1 | INTRODUCTION

Spontaneous blinking is a natural phenomenon that occurs ~15–20 times per minute (Tsubota, Kwong, Lee, Nakamura, & Cheng, 1999), with each blink lasting ~150–300 ms in duration (Manning, Riggs, & Komenda, 1983; Riggs, Volkman, & Moore, 1981). Though often considered within the physiological context of corneal lubrication, increasing evidence now suggests that the degree of cognitive

processing associated with blinking is greater than previously expected. Behavioral observations have demonstrated the modulation of blink rates by changes in attentional demand and cognitive load (Oh, Han, Peterson, & Jeong, 2012; Siegle, Ichikawa, & Steinhauer, 2008; Wascher, Heppner, Möckel, Kobald, & Getzmann, 2015), while functional magnetic resonance imaging (fMRI) findings have also pointed to the potential role of spontaneous blinking in modulating attentional mechanisms during cognitive behaviors (Nakano, Kato,

Morito, Itoi, & Kitazawa, 2013). Nonetheless, the neural processes underlying spontaneous blinking are still not well-understood.

Recent studies from electroencephalography (EEG) have reported electrophysiological signatures of blink-related neural processes known as blink-related oscillations (BROs), in which the brain exhibits increased activity following spontaneous blinking (Bonfiglio et al., 2013, 2014). BROs are believed to represent the cognitive processes associated with blinking, distinct from the well-known ocular and motor effects. The BRO response has mainly been described under resting conditions with or without passive fixation, and is particularly prominent in the delta frequency range (0.5–4 Hz). Specifically, the delta-band EEG amplitude and spectral power both exhibit increases following blink events, peaking at ~250–300 ms post-blink (Bonfiglio et al., 2009, 2013, 2014). A recent study in our group also demonstrated these temporal and spectral characteristics using magnetoencephalography (MEG), further validating the existence of BRO effects across different modalities (Liu, Ghosh Hajra, Cheung, Song, & D'Arcy, 2017). Moreover, studies have also pointed to the potential utility of the BRO response in clinical brain function assessments (Bonfiglio et al., 2013, 2014), with further possibility of deployment in bedside evaluations (Ghosh Hajra et al., 2016, 2018).

Crucially, previous MEG findings from our group further confirmed that delta BROs activated the bilateral precuneus regions known to be involved in environmental monitoring and self-awareness processes (Cavanna & Trimble, 2006; Liu et al., 2017). The precuneus is a critical hub within the default mode network (DMN), a network of brain regions exhibiting increased activity under rest-like conditions (Gusnard & Raichle, 2001; Hagmann et al., 2008). In fact, the precuneus/posterior cingulate cortex regions in particular have been found to be tonically active in the absence of goal-directed tasks, and these tonic precuneal activations are believed to represent the continual gathering of information from the environment (Raichle et al., 2001). Given the interruptions in visual input produced by spontaneous blinking, the observed increase in precuneal activity—above the tonic levels—following blink events is thought to represent *additional* environmental monitoring processes undertaken when the eyes close and reopen with each new blink (Bonfiglio et al., 2013, 2014; Liu et al., 2017). The fact that these processes occur as part of blinking at rest also confers possible evolutionary advantages, because the ongoing scanning of the environment for potential threat detection would likely have been necessary to compensate for the momentary loss of visual input due to blinking. In fact, it is possible that blink-related processing may be related to the phenomenon of vigilance for predator and threat detection in animals, as studies in primates have shown that the interblink intervals are correlated with the level of antipredator vigilance (Beauchamp, 2015; Matsumoto-Oda, Okamoto, Takahashi, & Ohira, 2018).

Although BROs have been reported under rest-like conditions, little is known about their effects during overt cognitive tasks. Yet the investigation of BRO responses under cognitive task conditions is crucial to validating the presumed association between BROs and blink-related cognitive processing, such that BRO responses should be observable across multiple task states and also show task-modulatory effects. This study aimed to investigate this issue using both passive fixation and cognitive task conditions.

Given the multitude of cognitive task possibilities (e.g., visual search, go/no-go, working memory, etc.), selecting the appropriate task for this study required consideration of the type and extent of cognitive loading and potential experimental confounds due to competing sensory or cognitive demands. As the focus of this study was the cognitive modulation of *blink*-related effects, the cognitive loading condition itself must be the background experimental factor, while the blink events occurring *during* the cognitive task will form the main effect of interest. As such, cognitive tasks that are known to engage some of the similar brain regions activated by BROs may be best suited to exert modulatory effects on BRO responses. In addition, the task should also require little sensory interaction with the environment to minimize potential experimental confounds due to simultaneous sensory processing. The task should be challenging so as to create sufficient cognitive loading to modulate BRO effects, but should not require active engagement of attentional resources in interacting with externally applied cues to minimize competing cognitive demands. In other words, the desired task should (a) be internally rather than externally focused; (b) engage similar brain regions compared to BROs; (c) require little or no sensory cues from the environment for task performance; and (d) avoid utilizing active attentional resources in interactions with the environment.

Mental arithmetic integrates many key cognitive processes such as magnitude comprehension, fact retrieval, calculation, sequencing, and visuo-spatial processing (Menon, 2010). Complex mental arithmetic tasks also require additional cognitive resources such as attention and working memory for the temporary storage and manipulation of information (Klein, Moeller, Glauche, Weiller, & Willmes, 2013). Mental arithmetic presented several key advantages as a potential task in this study: First, it may be performed internally in a serial fashion without repeated external instructional cues, such as in backward counting from a single starting value like 1,000. Second, greater complexity of calculations may be created by selecting specific counting step values with greater arithmetic difficulty, such as in counting by 7 (Stanislas Dehaene & Cohen, 1995; Fitzgibbon, Pope, Mackenzie, Clark, & Willoughby, 2004). In addition, mental subtraction in particular has been shown to activate several brain regions including the bilateral precuneus, which is of key interest in BRO responses (Fehr, Code, & Herrmann, 2007; Liu et al., 2017). Moreover, the external sensory environment may be easily controlled during task performance by instructing the participant to maintain visual fixation on an unchanging crosshair without the use of further sensory inputs, thereby mitigating potential experimental confounds due to extraneous sensory stimuli. Finally, the same cross-hair may be utilized in a passive fixation condition without any cognitive tasks to control for the effect of visual fixation. Thus, both the mental arithmetic and passive fixation tasks would involve identical sensory environments, but only mental arithmetic would contain a cognitive task. The cognitive modulation of BRO responses may then be evaluated by examining the effect of blink events during both these tasks.

Given the above considerations, this study investigated BRO characteristics in healthy individuals using MEG as they performed mental arithmetic and passive fixation tasks. We hypothesized that

- (a) BRO brain responses would be present during both tasks and
- (b) the BRO effects would be modulated by cognitive loading.

## 2 | MATERIALS AND METHODS

### 2.1 | Participants

Twenty-two healthy adults (age  $23.0 \pm 2.4$ , 9 female) participated in this study. All participants had normal or corrected-to-normal vision. This research was approved by the Research Ethics Boards of Simon Fraser University and Fraser Health Authority, and written informed consent was obtained from each volunteer prior to data acquisition.

### 2.2 | Experimental design

The experimental paradigm comprised two 10-min tasks, with the order counterbalanced across individuals. One task consisted of mental arithmetic (MA), in which participants were instructed to mentally count backwards from 1,000, subtracting 7 each time (i.e., 1,000, 993, 986, 979, etc.). Subjects were instructed to maintain visual fixation on a centrally presented crosshair (white on black background) throughout task performance, and to avoid moving their mouths or verbalizing the numbers. Instructions were also given for participants to restart the calculations at 1,000 if they forgot the current result at any point during the run. The other task consisted of passive fixation (PF), in which participants visually fixated on a crosshair identical to that used in MA, without any other stimulus or activities being performed.

Task compliance for MA was assessed through a combination of behavioral and neurocognitive effects, including verbal confirmation at the end of the run, offline evaluation of blink rate as a behavioral measure of cognitive load (Bentivoglio et al., 1997; Oh et al., 2012), source localization to confirm task-related cortical activations, and assessment of task-related spectral changes at both sensor and source levels.

### 2.3 | Data acquisition

Data acquisition took place in a well-lit, magnetically shielded room, with the participants resting comfortably in the supine position. Volunteers were not informed of the purpose of the study in order to acquire natural blink responses. MEG data were collected using a 151-channel CTF system (MEG International Services Ltd, Canada) with axial gradiometers (5 cm baseline) at 1,200 Hz sampling frequency. Synthetic third-order gradient noise cancelation was also applied. Continuous head location recording was made using head position indicator coils positioned at three fiducial points (nasion, left and right periauricular). Prior to data acquisition, the participant's head shape was measured using a 3D digitizer (Polhemus), and at least 500 points were acquired over the entire head. Blinks and eye movements were recorded using electrodes positioned near the left eye on the supraorbital ridge (vertical electrooculogram or vEOG) and outer canthus (horizontal EOG). Electrode impedances were kept below 5 k $\Omega$ . Data from the EOG channels were monitored online to ensure

that participants remained awake with their eyes open throughout the experiment, particularly during the PF task.

### 2.4 | Data preparation

#### 2.4.1 | EOG: Blink detection and behavioral evaluation

Blink detection and behavioral evaluations were performed using EOG data. Data were first visually inspected, then notch-filtered to remove power line noise, associated harmonics, and signal due to head position indicator coils. Subsequent blink detection and evaluation followed an automated template matching procedure in accordance with previously published methods (Bonfiglio et al., 2013; Liu et al., 2017). Briefly, data from the vEOG channel were band-pass filtered (0.1–30 Hz), and one blink template was manually selected for each dataset as best representing a stereotypical blink. The entire vEOG data were then convolved with the blink template, and potential blink instances were identified using the convolution signal by applying amplitude thresholding. To avoid contamination from activity due to other blinks, temporal thresholding was also applied to exclude any blink instances that were <3 s away from adjacent blinks. Data from 2 of the 22 participants were excluded from subsequent analyses due to frequent blinking, as none of the blink events in these individuals passed temporal thresholding. All final blink events were visually inspected to ensure artifact-free data. To facilitate behavioral evaluation, blink rate was measured prior to temporal thresholding to better capture complete blink behavior.

To enable quantitative assessment of blink behavioral characteristics across individuals, features were extracted from the vEOG recording that corresponded to different aspects of blink morphology (Figure 1a) (Bonfiglio et al., 2014; Liu et al., 2017). Features were derived at the individual level after averaging together all identified blink events, and compared at the group level using paired *t*-test to examine within-subject behavioral differences between the MA and PF tasks. Additionally, between-subject consistency in blink morphology was also evaluated for each task using a split-half approach as described previously (Liu et al., 2017). In particular, participants were randomly divided into two subgroups of equal size, and Pearson correlation was calculated after sorting the measurements in each group. This process was repeated 1,000 times following randomized group divisions, and the mean correlation coefficient was computed. The overall behavioral characteristics in each task were deemed to be consistent across individuals if the mean correlation coefficient exceeded 0.8 in accordance with previous literature (Luking, Nelson, Infantolino, Sauder, & Hajcak, 2017; Raz, Bar-Haim, Sadeh, & Dan, 2014).

Further to quantitative evaluations, qualitative comparisons were also made using the grand-averaged blink waveform for the two tasks (Figure 1a). The trial-averaged blink trace for each participant was first normalized relative to its own maximum amplitude prior to deriving the grand-average waveform, which helped to minimize bias at the group level due to potential large signals in raw blink amplitudes at the individual level.

#### 2.4.2 | MEG: Data preprocessing and segmentation

All subsequent analyses were performed on MEG data using a combination of EEGLAB (Delorme & Makeig, 2004) and SPM8 (Litvak et al.,

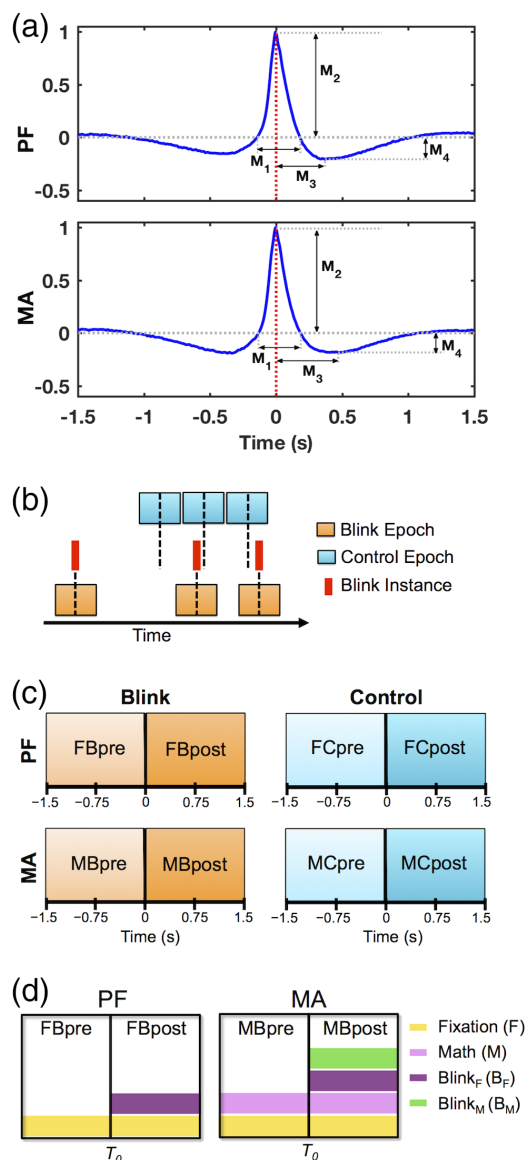


**FIGURE 1** Data preprocessing. (a) Grand average of 3 s blink epochs in vEOG data showing the quantitative morphological features used to evaluate behavioral characteristics across individuals. Features delineate the height and width of positive and negative regions within the blink trace.  $M_1$  = positive peak width;  $M_2$  = positive peak amplitude;  $M_3$  = negative peak time;  $M_4$  = negative peak amplitude. Red dotted line at 0 ms denotes the latency of maximum blink amplitude or  $T_0$ , corresponding to the moment of complete eye closure. (b) Schematic illustration of data segmentation technique. *Blink* epochs were centered on the latency of blink maximum ( $T_0$ ) for each blink event, while the *control* epochs were pseudo-random in timing with respect to blink instances. Number of trials was identical between *control* and *blink* conditions for each task and subject. Black dotted line represents time zero for each condition. (c) Schematic illustration of data segments used for statistical contrasts, corresponding to intervals before and after time zero for each condition and task. (d) Schematic illustration of key experimental factors in this study, applicable to the *blink* condition for PF and MA tasks. Rectangular boxes represent whole 3 s epochs, with central black lines denoting  $T_0$ . The effect of *fixation* (*F*) is common to both PF and MA tasks throughout the entire blink epochs, while the effect of *mental calculation* or *math* (*M*) is present throughout the epoch in MA. The effect of *blinking* has been decomposed into *blink<sub>F</sub>* (*B<sub>F</sub>*) and *blink<sub>M</sub>* (*B<sub>M</sub>*), representing *blinking* under *fixation* and *blinking* under

2011). Following visual inspection and removal of artifactual channels, MEG data were notch-filtered to remove power line noise and signal corresponding to head position indicator coils. Data were then band-pass filtered to 0.5–80 Hz, and independent component analysis (ICA) was performed using the *runica* algorithm (Makeig, Bell, Jung, & Sejnowski, 1996). Independent components corresponding to artifact (e.g., blinks, saccades, muscle contractions, cardiac activity, breathing) were removed.

To enable comparison with inherent brain activations that may not be time-locked to spontaneous blinks, an analytical control condition for non-time-locked activity was introduced at the data segmentation stage in accordance with previously published procedures (Liu et al., 2017). Specifically, data were segmented into 3 s epochs according to two conditions (Figure 1b): a *blink* condition centered on the latency of maximum blink amplitude or  $T_0$ , and a *control* condition comprising non-overlapping consecutive epochs that were pseudo-random in timing with respect to blink instances. The number of trials was matched between the *blink* and *control* conditions for each participant and task, and the *control* epochs were segmented near the middle of the 10-min datasets. The *blink* condition was used to elucidate main effects of interest with respect to BRO responses, while the *control* condition helped determine whether any observed BRO effects were blink-related rather than being the result of inherent brain activity.

### 2.4.3 | Statistical contrasts and experimental factors

Statistical contrasts were evaluated based on data from the intervals before and after time zero for each segmentation condition (i.e., *blink* and *control*) and experimental task (i.e., MA and PF) (Figure 1c). BRO responses were evaluated using four main experimental factors derived from the *blink* condition data (Figure 1d): (a) *Fixation* (*F*) corresponds to the effect of visual fixation on the crosshair, present in both MA and PF tasks and applicable to the entire epoch for each task; (b) *math* (*M*) corresponds to the effect of mental calculation, present in the entire epoch for the MA task; (c) *blink<sub>F</sub>* (*B<sub>F</sub>*) corresponds to the effect of *blinking during* fixation, present in both MA and PF tasks; and (d) *blink<sub>M</sub>* (*B<sub>M</sub>*) corresponds to the effect of *blinking during* calculation, present only in the MA task. Crucially, as previous studies had shown that blink-related effects were primarily present in the post-blink time windows (Bonfiglio et al., 2013, 2014; Liu et al., 2017), both blink-related factors were expected to impact mainly the respective post-blink intervals rather than the entire epoch.

Using these experimental factors, statistical contrasts were derived to examine various effects of interest (Table 1). Main BRO-related effects include blink-related increase in brain activity during the MA and PF tasks ( $\Delta_{MA}$  and  $\Delta_{PF}$ , respectively), as well as decreased blink-related processing in MA compared to PF ( $\Delta_{PF} - \Delta_{MA}$ ). Task-related effects in the absence of blink activity were evaluated by contrasting the *blink* condition data in the pre- $T_0$  interval between the

calculation, respectively. The former applies to both the PF and MA tasks as they both utilize visual fixation, while the latter applies only to the MA task. In both cases, the blink-related effects primarily manifest in the post-blink intervals

**TABLE 1** Statistical contrasts used to examine main effects of interest

	Effect of interest	Contrast	Experimental factors
$\Delta_{PF}$	Blink-related increase in PF task	FBpost – FBpre	$(F + B_F) - F = B_F$
$\Delta_{MA}$	Blink-related increase in MA task	MBpost – MBpre	$(F + M + B_F + B_M) - (F + M) = B_F + B_M$
$\Delta_{PF} - \Delta_{MA}$	Decreased blink-related processing in MA compared to PF	$(FBpost - FBpre) - (MBpost - MBpre)$	$B_F - (B_F + B_M) = -B_M$

MA and PF tasks (Supporting Information). Numerous additional contrasts were performed to investigate potential alternate BRO effects, such as blink-related decrease in activity and increased blink-related processing in MA relative to PF (Supporting Information). Furthermore, to ensure that any observed BRO effects were due to blink events rather than being part of inherent brain activity, comparisons were also made using the *control* condition data (Supporting Information).

#### 2.4.4 | Effectiveness of artifact removal

Prior to continuing analysis for potential blink-related effects, it is critical to first assess the effectiveness of the ICA-based artifact removal process. This multi-step evaluation was conducted following previously published methods (Liu et al., 2017), and is summarized below. First, the trial-averaged event-related fields (ERFs) for the *blink* condition data corresponding to each participant and task were visually inspected before and after artifact removal to confirm the elimination of signal features characteristic of ocular activity (e.g., “spikes” and “boxes”). Next, the spatial topographies for each dataset were examined at both blink maximum (0 ms latency) as well as preblink baseline (chosen to be –1,000 ms to maintain separation from potential saccadic eye movements associated with blink occurrence) to ensure that frontally concentrated signals were no longer present following artifact removal.

The subsequent stages involved quantitative analyses to examine the contribution of blink signal relative to that in the pre-blink baseline. Specifically, MEG sensors were first divided into regional subgroups according to location (i.e., frontal, central, parietal, temporal, and occipital), and a blink-to-baseline power ratio was computed for each region as follows:

$$\text{ratio} = \frac{\sum_{i=1}^n (y_i - \bar{y})^2}{\sum_{i=1}^n (x_i - \bar{x})^2}$$

where  $n$  is the number of channels in each region, and  $y_i$  and  $x_i$  are the ERF signal amplitudes at 0 and –1,000 ms latencies, respectively. This ratio provides information about the contribution of the maximal blink signal relative to the baseline signal in each region, while correcting for channel mean drifts. Ratios greater than unity thus denote increased contribution of ocular signals relative to baseline, while ratios below unity represent decreased contribution of ocular signals relative to baseline.

Using the power ratio measures, two sets of statistical analyses were subsequently undertaken to determine the impact of artifact removal. One analysis focused on the comparison of regional power ratios before and after artifact removal using paired *t*-test, providing information about the impact of artifact removal within each region. This was applied separately for each

experimental task (i.e., MA, PF) and data segmentation condition (i.e., *blink*, *control*). The other analysis examined cross-regional changes in power ratio using one-way repeated-measures analysis of variance (ANOVA), with *region* as a within-subject factor. This analysis was also performed separately for each condition and task, and enabled the assessment of potential statistical relationships among regions that may be consistent with the spatial propagation of ocular signal.

#### 2.5 | Overall effects

To provide an overview of both blink-related and task-related effects in different frequency bands, denoised continuous data were filtered into the delta (0.5–4 Hz), theta (4–8 Hz), alpha (8–12 Hz), beta (12–30 Hz), and gamma (30–80 Hz) frequencies, then segmented and trial-averaged to derive ERFs for each frequency band. Global field power (GFP) was computed from ERF signals, providing information about the demeaned signal power across all channels in each frequency band (Liu et al., 2017; Mitchell & Cusack, 2011; Skrandies, 1990). Individual-level mean GFP amplitudes were calculated by averaging over 1,200 ms intervals before (–1,500 to –300 ms) and after (0–1,200 ms) time zero for each task and segmentation condition. The resulting values were entered into group-level statistics using two-way repeated measures ANOVA, with *task* (i.e., MA vs PF) and *time* (i.e., pre- vs post- $T_0$ ) as within-subject factors. This analysis was conducted separately for each frequency band, with Bonferroni correction for any post-hoc comparisons. Additionally, as the *blink* and *control* conditions had been segmented “independently” with respect to blink instances—such that the *blink* condition reflected the presence of a time-locked experimental event while the *control* condition did not—separate analyses were performed for each segmentation condition. Outcomes from this overall analysis then informed subsequent analytical parameters.

#### 2.6 | BRO effects: Sensor activity

Building upon the previous ANOVA results, further analyses for BRO-related effects focused on the delta-band activity. The individual-level delta-band GFP waveforms were derived, and the mean GFP amplitudes were computed over a 200 ms time window in both pre- $T_0$  and post- $T_0$  intervals. The post- $T_0$  window was selected to span the maximum GFP amplitude (150–350 ms), while the pre- $T_0$  window was chosen to be –1,300 to –1,100 ms to represent preblink baseline activity. Statistical comparison was performed using paired *t*-test to evaluate potential changes in GFP amplitude following blink events. Identical time windows were used in all calculations, and separate analyses were conducted for each task and segmentation condition.

## 2.7 | BRO effects: Source localization

Source localization analysis followed previously published methods (Liu et al., 2017), and are summarized below. Briefly, standard forward modeling was performed using a single-shell spherical head model in SPM8, followed by source reconstruction using minimum norm estimates (Hauk, 2004). Group constraints were applied during inversion to improve source reliability across participants (Litvak et al., 2011; Litvak & Friston, 2008). Source reconstruction was based on denoised, segmented, and trial-averaged data (0.5–45 Hz) in the entire 3 s epoch (Liu et al., 2017). Time–frequency contrast images were generated by averaging the estimated source activity over the delta frequency band and across 200 ms time windows previously chosen based on delta-band GFP results, corresponding to the postblink GFP peak (150–350 ms) and the pre-blink baseline (–1,300 to –1,100 ms). These contrast images were then projected to a three-dimensional source space and smoothed using a Gaussian kernel with 8 mm full-width at half-maximum for input into statistical modeling. Statistical analysis employed a general linear model (GLM) using two-way ANOVA (Friston et al., 1994), with *time* (i.e., pre- $T_0$  vs post- $T_0$ ) and *task* (i.e., MA vs PF) as factors. Separate analyses were performed for the *blink* and *control* segmentation conditions. The differential blink rates between the PF and MA tasks were also incorporated as a covariate into the ANOVA design to account for potential interaction effects due to blink rate.

## 2.8 | BRO effects: Source activity

Given that the bilateral precuneus had been implicated in previous BRO studies as key regions of interest (Bonfiglio et al., 2013; Liu et al., 2017), further analysis was undertaken to examine source-level effects in these regions. Specifically, time course activity was extracted using virtual electrodes positioned at coordinates centered in activations clusters within the bilateral precuneus, particularly subregions of the posterior precuneus (pPC, MNI coordinates [–8 –76 46] and [10 –75 42]) and anterior precuneus (aPC, coordinates [–8 –44 67] and [10 –48 67]). For each virtual electrode, voxel time courses were smoothed over a spherical volume of interest with 5 mm radius, then filtered (0.5–45 Hz) and segmented following parameters in prior studies (Bonfiglio et al., 2014; Liu et al., 2017). Event-related spectral perturbation (ERSP) associated with blink events was derived using the continuous wavelet transform (CWT) with morlet function and 6 cycles (Makeig, 1993). CWT was computed for each virtual electrode and trial, and the log power was calculated as the logarithm of the squared absolute values of the wavelet coefficients. To evaluate blink-related effects, baseline correction was carried out by subtracting from each trial the mean log power during a preblink baseline window, selected to be –1,500 to –500 ms relative to  $T_0$  (Bonfiglio et al., 2013; Liu et al., 2017). Results were conditionally trial-averaged at the individual level, then grand-averaged across subjects. Statistical significance was assessed for each segmentation condition and experimental task using a bootstrapping approach. Specifically, group-level *T*-statistic values were first computed at each time point and frequency between data in the pre- and post-blink intervals. Data for each frequency were then randomly permuted

between the pre- and post-blink intervals, and new *T*-statistic values derived. Following 1,000 such randomized permutations of the data, a *T*-distribution was generated, and the actual *T*-statistic values were compared to this distribution in order to determine probabilities. Results were deemed significant if  $p < .05$ . A binary map of significance was also generated for all frequencies and time points in each task based on these probabilities, and the onset and offset latencies for the theta (4–8 Hz) and alpha (8–12 Hz) bands were extracted using the significant windows in this map.

## 2.9 | Task effects: Source activity

As the bilateral precuneus are also key cortical regions involved in mental calculation (Fehr et al., 2007), additional analyses were conducted to examine potential task-related effects in these regions. Similar to earlier BRO effect analysis, virtual electrode data were first extracted from the same cortical locations in pPC and aPC, filtered to 0.5–45 Hz, segmented, transformed using CWT, then averaged across trials for both *blink* and *control* conditions. For task-related comparison between MA and PF, mean log power during the pre-blink baseline in the PF task was subtracted from each time point of the corresponding condition in both tasks. Statistical significance was evaluated in a similar manner using bootstrapping, but comparisons were made between data in the MA and PF tasks within the same time windows. Separate analyses were conducted for each segmentation condition.

# 3 | RESULTS

## 3.1 | Data preparation outcomes

### 3.1.1 | EOG: Behavioral blink evaluation

Behavioral assessments using vEOG data showed that participants blinked more rapidly during the MA task compared to PF ( $p < .05$ , Table 2), consistent with increased cognitive load during MA (Bentivoglio et al., 1997; Oh et al., 2012). Additional quantitative analysis of blink morphological features showed no within-subject behavioral differences between the MA and PF tasks (Table 2). Further analysis of group-level behavioral consistency showed that correlations were extremely high across subjects for all morphological measures ( $r > .9$ ). These results demonstrate that blink behavior was highly consistent across individuals for both PF and MA tasks, and that the only difference observed was increased blink rate in MA as an indicator of cognitive load.

### 3.1.2 | MEG preprocessing: Effectiveness of artifact removal

Both qualitative and quantitative analyses demonstrated the efficacy of the artifact removal process. Visual inspection of individual-level ERF waveforms showed that spikes and box-like features consistent with ocular activity were eliminated following artifact rejection, with corresponding shifts in spatial topography from frontal eye to posterior regions (Figure 2a). Quantitative analysis of regional blink-to-baseline power ratios showed the presence of a significant *region* effect in the *blink* condition prior to artifact removal ( $F_{2,787,52,945} = 44.699$ ,

**TABLE 2** Behavioral characteristics derived from vEOG waveforms

	Measure name	MA		PF		Within-subject statistics $T_{19}$
		Raw	Correlation ( $r$ )	Raw	Correlation ( $r$ )	
	Blink rate (#/min)	15.00 ± 2.32	–	10.19 ± 1.44	–	2.325*
M <sub>1</sub>	Positive peak width (s)	0.327 ± 0.019	0.920 ± 0.056	0.336 ± 0.022	0.933 ± 0.042	–0.368
M <sub>2</sub>	Positive peak amplitude (μV)	46.91 ± 3.46	0.935 ± 0.039	45.63 ± 4.36	0.939 ± 0.037	0.427
M <sub>3</sub>	Negative peak time (s)	0.438 ± 0.024	0.909 ± 0.047	0.425 ± 0.026	0.945 ± 0.035	0.461
M <sub>4</sub>	Negative peak amplitude (μV)	–10.25 ± 1.37	0.926 ± 0.048	–10.99 ± 1.79	0.909 ± 0.058	0.565

Note. M<sub>1</sub>–M<sub>4</sub> are morphological features extracted from un-normalized, trial-averaged blink traces for each individual. *Raw* = measurements presented as mean ± standard error across individuals. *Correlation* = correlation coefficients from split-half analysis to determine between-subject behavioral consistency, presented as mean ± standard deviation across 1,000 repetitions. *Within-subject difference* = *T*-statistic values from paired *t*-test to determine within-subject differences in raw blink characteristics between the two tasks. \* $p < .05$

$p < .0001$ ), with reduction of power from the frontal and temporal regions towards the posterior areas in a pattern consistent with the spatial propagation of ocular signal (Figure 2b):

$$(\text{Frontal} \approx \text{Temporal})^* > (\text{Central} \approx \text{Parietal})^* > \text{Occipital},$$

where \* indicates  $p < .05$ .

However, this *region* effect was no longer significant following artifact removal ( $F_{4,76} = 2.190$ ,  $p = .078$ ), and the frontal-posterior spatial pattern associated with ocular activity also disappeared. There were significant reductions in power ratio in all regions following artifact removal ( $p < .001$ , Figure 2b), which was particularly prominent in the frontal and temporal areas where the ocular artifact was greater (98% and 99% power reductions, respectively).

Contrary to the *blink* condition outcomes, the *control* condition power ratios did not exhibit any significant *region* effects before or after artifact removal ( $F_{2,705,51,395} = 1.352$ ,  $p = .268$  before;  $F_{2,782,52,862} = 0.862$ ,  $p = .460$  after). Nor were there any significant changes in power ratios following artifact removal for any of the regions. These outcomes are consistent with expectations, as the *control* condition was not time-locked to blink events and was therefore not expected to have captured much blink activity.

### 3.2 | Overall effects: Sensor activity

Overall GFP analysis across different frequency bands showed that only the delta band *blink* condition data exhibited a significant main effect of *time* ( $F_{1,19} = 53.733$ ,  $p < .00001$ ), suggesting that significant changes in signal power occurred following blink events. This was not observed in the delta band *control* condition ( $F_{1,19} = 3.276$ ,  $p = .086$ ), or in any of the other frequency bands. Additionally, a significant main effect of *task* was observed in both the *blink* and *control* conditions for the gamma band ( $F_{1,19} = 4.743$ ,  $p = .042$  and  $F_{1,19} = 5.241$ ,  $p = .034$ , respectively), suggesting that both segmentation conditions captured MA task-related activity in this frequency band. Further non-significant, but potentially trending, task-related effects were observed in the theta ( $F_{1,19} = 4.082$ ,  $p = .058$  for *blink* condition;  $F_{1,19} = 3.618$ ,  $p = .072$  for *control* condition) and beta ( $F_{1,19} = 3.665$ ,  $p = .071$  for *control* condition) bands, along with a significant interaction effect in the beta band *blink* condition ( $F_{1,18} = 9.300$ ,  $p = .007$ ).

### 3.3 | Specific effects: Sensor activity

Further evaluation of BRO effects focused on delta-band GFP activity, with the *blink* condition results showing increased power in the post-blink interval compared to pre-blink in both MA and PF tasks, each peaking at ~250 ms latency (Figure 3a, *top*). This effect was absent in the *control* condition. The increase in *blink* condition GFP amplitudes was statistically significant in both tasks ( $p < .0001$ , Figure 3a, *bottom*). There was also an apparent increase in the *blink* condition peak amplitudes between PF and MA tasks, but this was not statistically significant ( $T_{19} = 1.360$ ,  $p = .190$ ). Additional comparisons revealed task-related increase in gamma-band GFP amplitude in MA compared to PF task, occurring in both the *blink* and *control* conditions ( $p < .05$ , Figure 3b).

### 3.4 | BRO effects: Source localization

Source localization in the delta band showed blink-related activations in the bilateral occipital, posterior parietal, and anterior temporal regions during the PF task ( $p < .001$  *unc.*, Figure 4  $\Delta_{PF}$ ). Activation was also observed in the bilateral lingual and fusiform gyri along with the right parahippocampal gyrus. In comparison, blink-related activations during MA were decreased in extent compared to PF, with reductions visible across the occipital, posterior parietal, and temporal regions and particularly prominent in the right-hemisphere ( $p < .001$  *unc.*, Figure 4  $\Delta_{MA}$ ). Additionally, BRO-related activation of the lingual, fusiform, and right parahippocampal gyri also disappeared during MA. While both tasks showed blink-related activation of the bilateral precuneus, the extent of precuneal activations—particularly in the anterior subregion—was reduced in MA compared to PF ( $p < .001$  *unc.*, Figure 4  $\Delta_{PF} - \Delta_{MA}$ ). Interestingly, blinking during MA also activated the right inferior frontal gyrus (IFG) and supramarginal gyrus (SMG) ( $p < .001$  *unc.*, Figure 4  $\Delta_{MA}$ ).

To evaluate the potential alternative BRO effects and ensure that any observed BRO effects were due to blink events rather than inherent brain activity, numerous other contrasts were also examined (Supporting Information). No suprathreshold activations were found in any of these contrasts. Additionally, task-related effects in the absence of blink activity were also confirmed (Supporting Information), and no interaction effects were found for the differential blink rates between the MA and PF tasks.

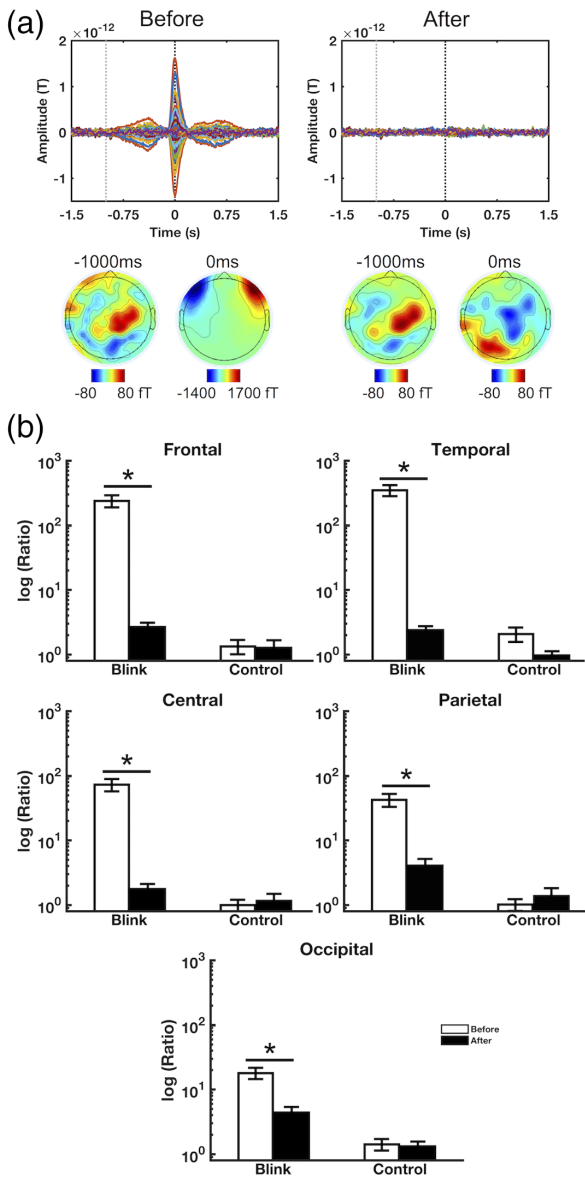


**FIGURE 2** Artifact removal results. (a) Representative subject data showing all-channel ERFs and spatial topographies before and after artifact removal. Signal characteristics consistent with ocular activity disappear following artifact removal. Black and gray dotted lines denote the latencies corresponding to maximum blink amplitude (0 ms) and pre-blink baseline (−1,000 ms), respectively. (b) Regional blink-to-baseline power ratios before and after artifact removal, calculated for each subject and presented as mean  $\pm$  SE across subjects. Results shown in log scale due to the high discrepancy between values. Data shown for MA task; PF task data are presented in Supporting Information. \* $p < .001$

### 3.5 | BRO effects: Source activity

Source activity in the bilateral pPC demonstrated increased spectral power in the delta and beta/gamma frequency bands in the first 300 ms following blink events, representing event-related synchronization (ERS) of oscillatory activity compared to the pre-blink interval ( $p < .05$ , Figure 5, top). This was followed by prolonged reduction in spectral power in the theta and alpha bands ( $p < .05$ ), or event-related desynchronization (ERD). These effects occurred in the blink condition

in both PF and MA tasks, but were absent in the control condition (Supporting Information, Figure 4). Interestingly, the latency of onset in the theta and alpha ERD also differed between the two tasks (Figure 5, bottom). Comparison of their respective windows of significance showed a bilateral earlier onset of the alpha ERD in MA (~60 ms and ~30 ms in left and right pPC, respectively), accompanied by an earlier offset in the left pPC (~160 ms). In contrast, theta ERD was delayed in MA in the left pPC (~100 ms), but had slightly earlier latency in the right pPC (~20 ms). Moreover, theta offset was unchanged in MA within the left pPC, but was ~160 ms earlier in the right pPC.

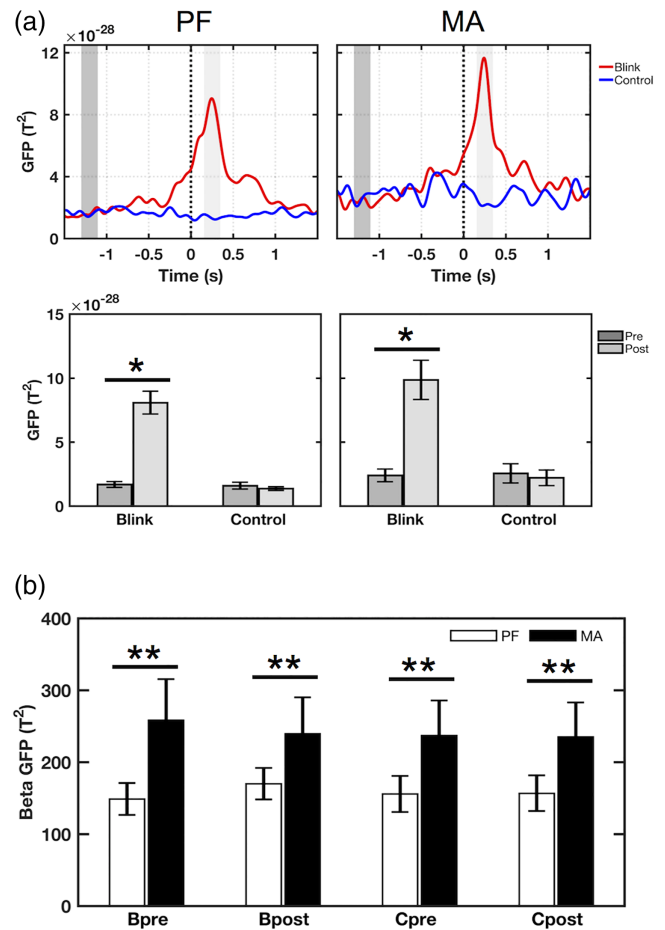


**FIGURE 3** GFP results in the delta and gamma bands. (a) Delta-band results. Top: Grand-averaged GFP waveforms showing increased GFP amplitude in the blink condition, peaking at approximately 250 ms post- $T_0$  for both MA and PF tasks. This is not seen in the control condition. Black dotted line denotes  $T_0$ . Dark- and light-gray shaded regions represent 200 ms windows of interest in the pre- $T_0$  and post- $T_0$  intervals, respectively. Bottom: Mean GFP amplitude for the corresponding tasks, averaged over the highlighted windows of interest. Measurements were computed for each individual and presented as mean  $\pm$  SE across subjects. Identical windows were used for both tasks. \* $p < .0001$  paired  $t$ -test. (b) Gamma-band results showing mean GFP amplitude in the intervals before (−1,500 to −1,300 ms) and after  $T_0$  (0–1,200 ms). Both blink and control conditions show increased gamma power in MA compared to PF. Bpre = blink condition pre- $T_0$ ; Bpost = blink condition post- $T_0$ ; Cpre = control condition pre- $T_0$ ; Cpost = control condition post- $T_0$ . \*\* $p < .05$  paired  $t$ -test



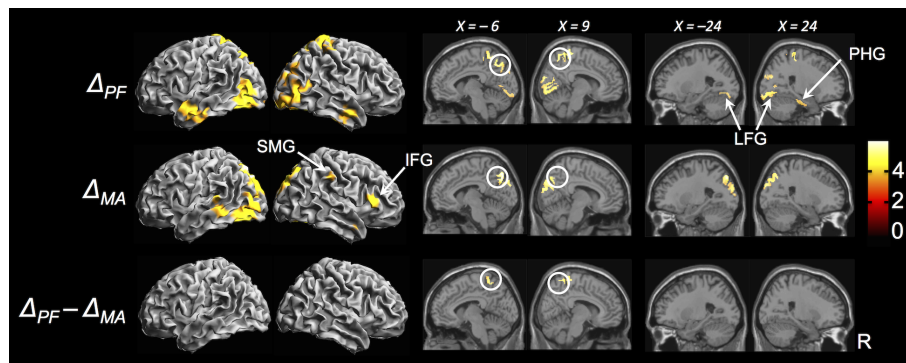


**FIGURE 4** Source localization results ( $p < .001$  *unc.*,  $k = 20$  voxels).  $\Delta_{PF}$  = blink-related increase in activity in PF task;  $\Delta_{MA}$  = blink-related increase in activity in MA task;  $\Delta_{PF} - \Delta_{MA}$  = decreased blink-related activation in MA compared to PF; color bar represents T-statistic values. White circles denote precuneus activation. SMG = supramarginal gyrus; IFG = inferior frontal gyrus; LFG = lingual and fusiform gyri; PHG = parahippocampal gyrus. Coordinates in MNI space

### 3.6 | Task effects: Source activity

Following earlier results demonstrating reduced blink-related activation in the bilateral aPC between the PF and MA tasks (Figure 4  $\Delta_{PF} - \Delta_{MA}$ ), investigation of task-related effects in these regions showed that the bilateral aPC exhibits a similar ERS/ERD pattern relative to that of the pPC, but only during the PF task in the *blink* condition. This pattern is not observed in the *control* condition during PF task, or in either condition during the MA task. Instead, there was bilateral increase in theta and beta/gamma band power in both *blink* and *control* conditions during the MA task, which was more prominent in the right aPC.

## 4 | DISCUSSION

This study utilized MEG to investigate blink-related oscillations under both MA and PF tasks in order to elucidate potential cognitive modulations of BROs. As BRO effects have thus far only been described under resting and passive fixation conditions, the evaluation of this response under cognitive loading conditions represents an important step forward in validating the presumed association between BROs and cognitive processing. We hypothesized that (a) BRO brain responses would be present during both MA and PF tasks, and (b) BRO effects would be modulated by cognitive loading.

### 4.1 | Main findings

#### 4.1.1 | Hypothesis 1: BROs present in both tasks

Our findings confirmed the presence of BRO brain responses during both MA and PF tasks, with characteristics that are similar across both tasks. In particular, we demonstrated that: (a) BROs during both tasks showed blink-related increase in GFP magnitude peaking at  $\sim 250$  ms post-blink (Figure 3a); (b) BROs during both tasks demonstrated blink-related activation of the bilateral precuneus regions as well as regions of the occipital, inferior temporal, and posterior parietal cortices (Figure 4  $\Delta_{MA}$ ,  $\Delta_{PF}$ ); and (c) BRO responses in both tasks were observed only in the *blink* segmentation condition and were absent in *control*, indicating that effects were time-locked to blink events and were not due to inherent brain activity. These results are all consistent

with previous reports of BRO effects under resting and passive fixation conditions (Bonfiglio et al., 2013; Liu et al., 2017), and provide further evidence in establishing the validity of this response across multiple task states.

#### 4.1.2 | Hypothesis 2: BROs modulated by cognitive loading

In comparing the BRO responses between the MA and PF tasks, this study also observed several key differences in BRO effects which suggest that this response is modulated by cognitive loading: (a) Blink-related activation of the bilateral precuneus was decreased in MA compared to PF (Figure 4  $\Delta_{PF} - \Delta_{MA}$ ); (b) blink-related activation of the fusiform, lingual, and right parahippocampal gyri were observed during PF but was absent in MA (Figure 4); (c) blinking did not activate the right SMG and IFG regions during the PF task, but did activate these regions during MA (Figure 4); and (d) BRO-induced spectral effects were observed in both MA and PF tasks in the posterior precuneus (Figure 5), but these effects disappeared in the anterior precuneus in MA (Figure 6). All BRO-related effects were observed only in the *blink* segmentation condition and were absent in the *control* condition, indicating that these effects were blink-related rather than part of inherent brain activity. Together, these results further extend previous findings regarding BRO responses by elucidating the differential characteristics of this phenomenon under alternate cognitive loading conditions.

### 4.2 | Study implications

#### 4.2.1 | Methodology

As the objective of this study was to investigate the differential effects of BROs during the MA and PF tasks, the results were focused on *blink*-related rather *task*-related activity. Although the primary experimental factor under manipulation was the use of MA or PF task, the main effects of interest were the blink events occurring *on top of* these tasks—in other words, the main results focused on the blink events as modulated by the cognitive loading conditions associated with the MA or PF tasks. It is important to note that, because both tasks used identical sensory environments and the mental subtraction in MA was performed internally in a serial fashion without repeated

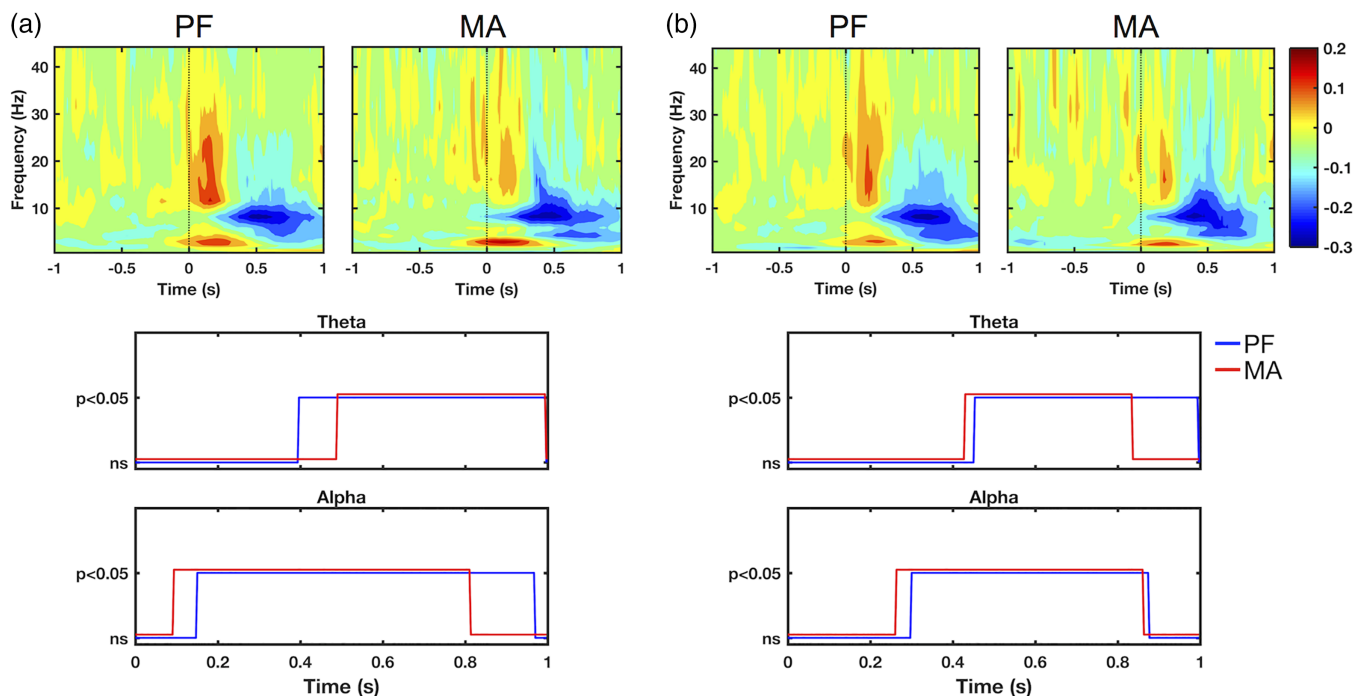


**FIGURE 5** Source-level wavelet spectral power demonstrating blink-related effects in the left (a) and right (b) pPC. Results are shown for *blink* condition only. *Top panels:* Grand-averaged log spectral power from ERS analysis. Black dotted line denotes  $T_0$ . Color bar represents log power values. *Bottom panels:* Statistical significance relative to pre-blink baseline in the alpha and theta frequency bands. Horizontal axes denote time relative to  $T_0$ . Vertical axes represent statistical test outcomes. ns = not significant

external cues, only calculation-induced cognitive loading should have been the driving factor behind differential effects observed between the MA and PF tasks. As such, comparison between the blink-related activities in both tasks (i.e.,  $\Delta_{MA}$  vs  $\Delta_{PF}$ ) should help elucidate potential modulatory effects of mental calculation on BRO responses.

#### 4.2.2 | Reduction of BRO-related cortical activations under cognitive loading

BRO-related activation of the precuneus is believed to represent environmental monitoring processes associated with spontaneous blinking, as the brain examines each new image that appears before the eyes following eye reopening (Bonfiglio et al., 2013, 2014; Liu et al., 2017). Though these findings have previously been reported for only resting and passive fixation conditions, this study now demonstrates BRO-related activation of the precuneus regions in both MA and PF tasks, thus extending the previous findings towards cognitive task conditions. Additionally, we also observed the reduction of BRO-related precuneal activation in MA compared to PF (Figure 4  $\Delta_{PF} - \Delta_{MA}$ ), which is consistent with the activation of this region during mental arithmetic processing—particularly in subtraction tasks (Fehr et al., 2007; Kong et al., 2005). As both blinking and mental arithmetic are known to activate the precuneus regions—and blinking was a secondary factor in MA on top of ongoing calculations—the simultaneous engagement of the precuneus region in calculation task performance likely contributed to the reduction of BRO-induced precuneus activation during this task. These findings help to validate the involvement of the precuneus regions in BRO effects. Additionally, these results are also consistent with the influential triple-code model of numerical cognition, in which the bilateral intraparietal sulcus areas (with medial

extensions into the precuneus) are believed to represent numerical magnitude information crucial in mental calculations (Dehaene & Cohen, 1995; Dehaene, Piazza, Pinel, & Cohen, 2003).

In addition to the precuneus, further reductions of BRO-related cortical activations were also observed across other occipital and temporal regions in MA compared to PF, including the complete disappearance of BRO-related lingual and fusiform activations during MA (Figure 4  $\Delta_{PF}$ ,  $\Delta_{MA}$ ). BRO-induced activation of lingual and fusiform gyri during PF is consistent with previous reports (Berman, Horowitz, Morel, & Hallett, 2012; Bonfiglio et al., 2014; Liu et al., 2017), and may be related to sensory processing of blink-related information as these regions have been previously linked with visual processes including complex image encoding, face perception, and object recognition (Bar et al., 2001; Machielsen, Rombouts, Barkhof, Scheltens, & Witter, 2000; Weiner & Zilles, 2016). On the other hand, the absence of these activations during MA may be due to the involvement of these regions in the competing task of mental calculation. In particular, the triple-code model postulates that visual recognition of number forms is subserved by occipital regions along with the lingual and fusiform gyri (Dehaene, Molko, Cohen, & Wilson, 2004), while verbal representation of numbers is associated with left-lateralized perisylvian areas (Grabner et al., 2009). This has been further substantiated by studies reporting differential activation patterns when participants solved mental arithmetic problems using different calculation strategies (i.e., visualization vs verbalization of numbers) (Ischebeck et al., 2006; Zarnhofer et al., 2012, 2013). Since participants in this study were instructed to perform mental calculations internally without moving their mouths, they may have been more likely to employ a visualization strategy that recruits occipital, lingual, and fusiform

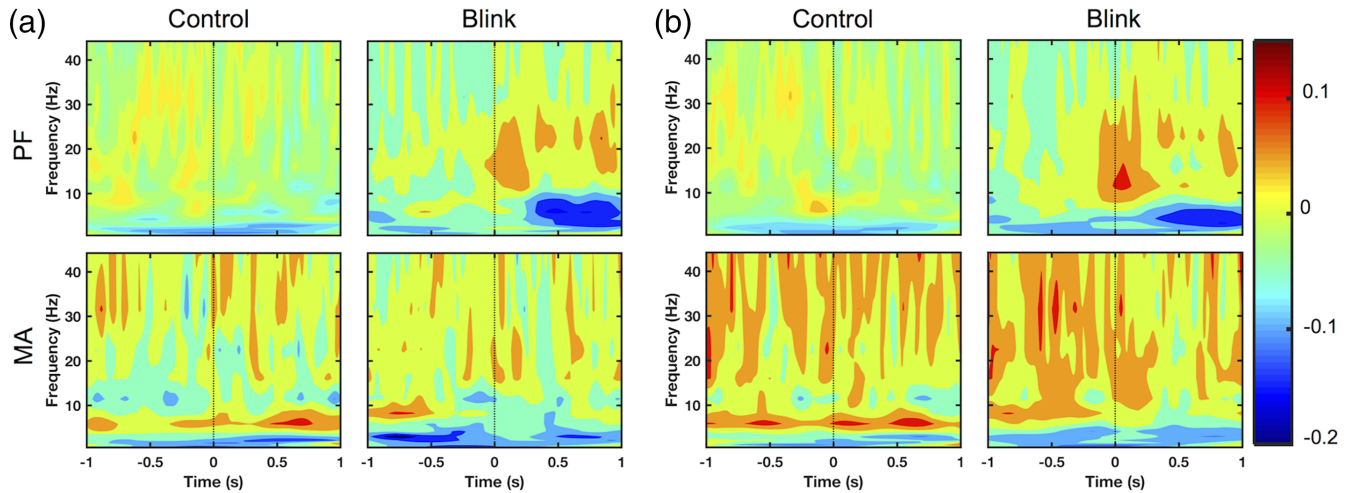


**FIGURE 6** Source-level wavelet spectral power demonstrating task-related differences in the left (a) and right (b) aPC. The ERS/ERD pattern seen in the *blink* condition during PF task is not found in the *control* condition. MA task shows right-lateralized increase in theta and beta/gamma power for both *blink* and *control* conditions. Black dotted line denotes  $T_0$ . Color bar represents log power values

regions. Hence, the disappearance of these activations as part of BRO-induced effects during MA may have been the result of competing task demands due to mental calculation. Nonetheless, this interpretation remains tentative, as this study did not directly investigate the impact of different calculation strategies. Future work is needed to better elucidate these effects.

Similar task-induced reduction of BRO-related activity was also observed in the right parahippocampal gyrus, which exhibited blink-related activation in PF but not in MA (Figure 4  $\Delta_{PF}$ ,  $\Delta_{MA}$ ). The activation of this region under PF is consistent with previous reports of blink-related brain activity (Berman et al., 2012; Bonfiglio et al., 2014; Liu et al., 2017). Parahippocampal activations have also been reported in previous studies investigating visuospatial processing using tasks such as viewing of natural scenes and landmarks (Aminoff, Kveraga, & Bar, 2013; Epstein & Kanwisher, 1998; Epstein & Ward, 2010; Park & Chun, 2009) and spatial navigation (Aguirre, Detre, Alsup, & D'Esposito, 1996; Mellet et al., 2000). Additionally, other studies examining associative episodic memory (wherein different items are bound together to form a compound construct or episode) have also demonstrated parahippocampal activations (Aminoff et al., 2013). These memory studies utilized stimulus paradigms containing face-name pairs (Kirwan & Stark, 2004), objects with associated contexts (Davachi, Mitchell, & Wagner, 2003), and paired items featuring faces alongside spatial or nonspatial information (Duzel et al., 2003). In interpreting these findings, it has been proposed that the parahippocampal regions act as an important conduit in the medial temporal lobe memory system by first processing spatial and nonspatial information in its posterior and anterior portions, respectively, then feeding this information to the hippocampus where they are merged to form cohesive representations of the object and associated context (Dickerson & Eichenbaum, 2010). Building upon this, another influential theory postulates that the primary function of the parahippocampal cortex is to process contextual associations in both spatial and nonspatial domains (Aminoff et al., 2013). These associations are believed to be formed by repeated exposures to prototypical

clustering of objects (e.g., “oven” and “sink” objects within a “kitchen” context), and helps to reconcile the dual roles of the parahippocampal cortex in both visuospatial processing and associative episodic memory (Aminoff et al., 2013). Specifically, visuospatial associations are ascribed to the spatial relationships of objects with their environment (e.g., *layout* of the cabinets in a kitchen), while episodic memory associations are attributed to the binding together of items that belong to the same episode (e.g., *dishes* are usually *washed* at the kitchen *sink*) (Aminoff et al., 2013).

In this study, BRO-induced activations in the PF task spanned portions of both anterior and posterior parahippocampal regions and a part of the hippocampus (Supporting Information, Figure 6). This pattern of activation overlaps with those previously reported in both visuospatial processing as well as associative episodic memory studies (Kirwan & Stark, 2004; Park & Chun, 2009), suggesting possible involvement of memory as well as contextual association processes in the BRO response (Aminoff et al., 2013; Dickerson & Eichenbaum, 2010). However, this finding is somewhat unexpected given our study did not utilize any active stimulus to prime the encoding/retrieval or association processes. Indeed, the only sensory input employed in the current study comprised a visual fixation cross that remained unchanged throughout the session. Nonetheless, given the momentary loss of visual input occurring with each blink instance, it is possible that the consequent disappearance and reappearance of the fixation cross may have created the effect of a “new” visual stimulus to be processed. This interpretation is in line with the aforementioned theory of contextual association processing in parahippocampal activations, which requires repeated exposures to a “prototypical context” to form the associations (Aminoff et al., 2013). In this case, the multiple closing and re-opening of the eyes with blink events may have produced repeated exposures to the visual fixation cross (i.e., black cross on white background) as an “object”. This “object” would then be evaluated with respect to its spatial associations (i.e., fixation cross is located at *center* of screen) as well as its nonspatial associations (i.e., fixation cross is *black* on *white* background). It is important to

note that these association-related parahippocampal activations occur even in the absence of active encoding/retrieval tasks, as previous work has demonstrated that *passive viewing* of visual information containing contextual associations also elicited parahippocampal effects (Bar, Aminoff, & Schacter, 2008). Thus, we speculate that the blink events in our study may have somehow created the effect of a passive visual stimulus from the fixation cross, but further studies are needed to validate these interpretations.

Although our results showed blink-related parahippocampal activations in PF, no such activations were observed in MA. This is consistent with the involvement of parahippocampal regions in mental calculation (Fehr et al., 2007; Menon, 2010). Given the expected competing effects between calculation and blinking in the MA task, these findings suggest that activation of the parahippocampal regions for blink processing is also dependent on the availability of cognitive resources in light of other task demands.

#### 4.2.3 | BRO-induced activation of ventral attention network regions during cognitive loading

An interesting finding in this study is the unexpected observation that blinking during MA also activated the right SMG and IFG regions (Figure 4  $\Delta$ MA). These regions are consistent with areas of the ventral attention network (VAN) involved in stimulus-driven attention and the detection of behaviorally relevant sensory stimuli, particularly when the stimuli are salient or unexpected (Corbetta & Shulman, 2002). As this study did not utilize any active external stimulus aside from an unchanging crosshair that was identical between the MA and PF tasks, we did not expect the activation of stimulus-driven attention in either task. Nonetheless, the decrease in BRO-induced occipital, temporal, and precuneal activations in the MA task compared to PF suggests a potential reduction of neural resources for blink processing under mental calculation conditions. As such, the activation of VAN regions during MA suggests the possible recruitment of additional cognitive resources for blink processing during the cognitive task. Thus, the observed activation patterns suggest that during cognitive task conditions, the brain may be making additional efforts to scan the environment with each eyeblink to detect any unexpected but potentially salient events. This interpretation is also consistent with the environmental monitoring and self-awareness aspects of blink-related brain activations, as the brain must be able to detect salient inputs and reorient attention where needed—particularly when attention is already engaged in another task.

In light of the observed blink-related activation of VAN regions during the MA task, we speculate that the cognitive loading conditions underlying blink events may play a role in modulating the BRO-induced activation of VAN regions. This is supported by our observation that blinking during PF activated the visuospatial pathways involving the parahippocampal, lingual, and fusiform gyri among others, while blinking during MA activated the VAN regions but not the visuospatial pathway areas. Nonetheless, further studies are needed to better elucidate the relationship between cognitive loading and blink-related activation of VAN regions.

#### 4.2.4 | BRO-related spectral differences under cognitive loading

Following the observation that the task-induced disappearance of BRO-related precuneal activation was primarily concentrated in the anterior rather than posterior portion of the precuneus, we further investigated the *blink* condition spectral effects in both subregions. Our findings revealed that the pPC exhibited a similar pattern of blink-related spectral effects during both MA and PF tasks with accompanying cortical activations (Figures 4 and 5), while the aPC showed this pattern and associated cortical activations during the PF task but not during MA (Figures 4 and 6). The BRO-related spectral pattern comprised an early ERS in the delta and beta/gamma bands during the first ~300 ms post-blink, followed by a later and more prolonged ERD in the theta and alpha bands. Given these observations, we postulate that this ERS/ERD pattern may represent potential neurocognitive mechanisms associated with blink-related processing in the precuneus.

In interpreting the pattern of ERS/ERD activity, previous literature has postulated that beta/gamma oscillations during the initial 400 ms post-stimulus interval may represent visual processing and sensory perception (Tan, Lana, & Uhlhaas, 2013), as studies have shown that their amplitudes correlate with stimulus properties such as contrast, duration, and size (Perry, Hamandi, Brindley, Muthukumaraswamy, & Singh, 2013; Schadow et al., 2007). In addition, alpha oscillations are believed to represent inhibitory processes in the brain, such that reduction of alpha (i.e., alpha ERD) leads to increased excitatory capacity of neuronal populations—and reflects active information processing (Jensen & Mazaheri, 2010; Klimesch, 2012; Klimesch, Sauseng, & Hanslmayr, 2007). In fact, brain regions activated during a task have been shown to exhibit alpha ERD, while task-irrelevant areas exhibit alpha ERS (Foxe, Simpson, & Ahlfors, 1998; Kelly, Lalor, Reilly, & Foxe, 2006; Sauseng et al., 2009; Thut, Nietzel, Brandt, & Pascual-Leone, 2006). Finally, theta-band power reductions have been observed in tasks involving successful encoding of episodic and associative memory (Greenberg, Burke, Haque, Kahana, & Zagh-loul, 2015; Matsumoto et al., 2013).

Based on these findings in prior literature, we tentatively postulate a potential mechanism for blink-related processing in the brain, comprising an early sensory response to new visual information produced by blink events (i.e., beta/gamma ERS), followed by later and more prolonged responses related to information processing and episodic memory (i.e., theta and alpha ERD). In this context, the observed alpha ERD may represent increased excitability of neurons in order to facilitate information processing. Similarly, the earlier delta ERS may also be associated with long-range cortical communications in facilitating these mechanisms (He & Raichle, 2009). Thus, the early beta/gamma ERS effect potentially corresponds to relatively low-level sensory processes, while the ERD components may represent high-level cognitive processes. Crucially, this proposed mechanism is also consistent with the pattern of BRO-related cortical activations observed in this study: the occipital, posterior parietal, and anterior temporal regions span the dorsal and ventral visual streams (Hebart & Hesselmann, 2012); the precuneus region has been associated with environmental monitoring as well as episodic memory processes (Cavanna &

Trimble, 2006); and the parahippocampal gyrus has been implicated in episodic memory and visuospatial processes (Aminoff et al., 2013).

As this study also observed task-related differences with respect to the latency of theta and alpha ERD in the pPC, it is important to examine interpretation of these findings in light of the proposed neural mechanism. In particular, if the alpha ERD is related to release of inhibition in preparation for blink-related information processing, then the earlier onset latency of the alpha ERD in MA relative to PF may represent “additional efforts” made by the brain to process blink-related information when the brain is already engaged in a competing mental arithmetic task. In other words, the brain must act earlier to prepare itself to process blink-related information during high cognitive loading conditions. This is also supported by the fact that mental calculation is known to engage the precuneus regions (Fehr et al., 2007), which during the MA task must undertake *both* calculation *and* BRO processing. Similarly, the earlier offset of the alpha ERD in the left posterior precuneus during MA may represent the brain's attempt to quickly complete any blink-related processing in order to return to the cognitive task at hand. Additionally, theta ERD latencies also showed task-related differences between the left and right pPC, although the underlying mechanism for this cross-hemispheric difference is unclear. We speculate that this may be related to the lateralization of precuneal activations sometimes observed in subtraction mental arithmetic tasks (Kong et al., 2005), but further studies are needed to better elucidate these effects.

While a previous study by Bonfiglio et al. also reported blink-related ERS/ERD in the alpha band (Bonfiglio et al., 2011), it is important to note that key methodological advantages distinguish our study in comparison. First, Bonfiglio et al. employed a 19-channel EEG system with an average-reference scheme, while our study utilized a 151-channel MEG system with reference-free recording. As average referencing requires both a high electrode density and large scalp surface coverage, the use of low-density EEG with this scheme is known to produce spurious alpha effects (Hagemann, Naumann, & Thayer, 2001). Moreover, EEG also has inherent limitations due to electrical field distortions in volume conduction (Nunez et al., 1994), while MEG is much less susceptible to this effect given that the propagation of magnetic fields is not impacted by differences in tissue conductivity (Marinova & Matee, 2010). Finally, the techniques used to examine the alpha-band effects differ significantly between the two studies, as Bonfiglio et al. reported the *sensor-level* ERS/ERD effects, while our study examined *source-level* spectral effects within the precuneus region. Our approach thus provides a more direct evaluation of precuneus activity compared to the previous study.

A previous fMRI study examining the effect of spontaneous blinking while viewing videos also reported blink-related activation of the bilateral hippocampal regions (Nakano, 2015). This is in line with the blink-related parahippocampal activations and theta-band effects observed in this study, as theta oscillations are known to be associated with hippocampal and parahippocampal activity, particularly in the context of memory-related processes (Buzsáki, 2002; H. Zhang & Jacobs, 2015). Nonetheless, it should be noted that the low temporal resolution of fMRI in the previous study renders it a less than ideal method for examining blink-related brain activity, as fMRI results are derived from neural hemodynamic responses occurring on the order

of *seconds*, while the time course of spontaneous blinking is on the order of *milliseconds*. In light of this, results from this MEG study provide important new insights into neural activity occurring with each blink instance and on the same time scale.

Although a beta-band interaction was observed in sensor space GFP, further analyses did not reveal any specific effects that were statistically significant (Supporting Information, Section V). More studies are needed to further explore beta-band effects in BRO responses.

#### 4.2.5 | Task-related effects

While the pPC showed primarily BRO-related spectral effects with relatively few task-related differences, more task-related effects were observed in the aPC. Although this region exhibited a similar ERS/ERD pattern reminiscent of BRO processing in the PF task, no such pattern was present in MA. Instead, there was increased theta and gamma band power throughout the epoch in both *control* and *blink* conditions. These effects are consistent with the task-related increase in sensor-space gamma and theta power observed in our study (Table 3), and are also consistent with the increased gamma and theta power previously reported for mental arithmetic tasks (Fitzgibbon et al., 2004; Ishii et al., 2014). Additionally, further contrasts were also performed to examine the presence of task-related cortical effects in the absence of blink activity (Supporting Information, Table 3). Results showed that MA led to increased activation of the right precuneus, dorsolateral prefrontal cortex, and angular gyrus regions (Supporting Information, Figure 3), which are consistent with mental arithmetic processing (Fehr et al., 2007; Klein et al., 2013). As challenging mental arithmetic tasks are also known to engage working memory resources (Menon, 2010), the activation of dorsolateral prefrontal cortex is also consistent with the engagement of working memory during the calculation task (Chai, Abd Hamid, & Abdullah, 2018). Together, these findings confirm the task-related effects in MA relative to PF, and suggest that there may be a functional separation between the pPC and aPC subregions in BRO processing under mental arithmetic-based cognitive loading. Whereas the pPC continues to perform blink-related processing during MA, the aPC is preferentially allocated for calculation task performance, and no longer undertakes blink-related processing during the task.

The observed functional segregation of the posterior and anterior precuneus may be related to potential differences in structural and functional connectivity between these regions. The precuneus as a whole possesses strong anatomical and functional connections with the occipital, prefrontal, thalamic, and hippocampal regions of the brain (Cunningham, Tomasi, & Volkow, 2017; Zhang & Li, 2012). However, functional connectivity differences have also been reported among various precuneal subregions, such that the ventral region adjacent to the posterior cingulate cortex is believed to be positively correlated with the resting-state DMN network (Buckner, Andrews-Hanna, & Schacter, 2008; Pfefferbaum et al., 2011), while the dorsal precuneus is correlated with the superior parietal and other areas not part of the DMN (Zhang & Li, 2012). These reports are in line with the results of this study showing cortical activations of the dorsal rather than ventral precuneus regions for blink and calculation processing.

**TABLE 3** Overall effects in sensor-level GFP for each frequency band

		$\delta$ (0.5–4 Hz)	$\theta$ (4–8 Hz)	$\alpha$ (8–12 Hz)	$\beta$ (12–30 Hz)	$\gamma$ (30–80 Hz)
Time ( <i>Post vs Pre T<sub>0</sub></i> )	C	ns	ns	ns	ns	ns
	B	$p < .0001$	ns	ns	ns	ns
Task ( <i>MA vs PF</i> )	C	ns	$p = .072$	ns	$p = .071$	$p = .034$
	B	ns	$p = .058$	ns	ns	$p = .042$
Interaction ( <i>task × time</i> )	C	ns	ns	ns	ns	ns
	B	ns	ns	ns	$p = 0.005$	ns

Note. Abbreviations: B = *blink*; C = *control*; ns = not significant.

Results show probabilities from the omnibus two-way repeated measures ANOVA with *time* and *task* as within-subject factors.  $p < .05$  is considered to be significant.

In addition to the dorsal–ventral differences, studies have also reported further segregation in functional connectivity within the dorsal precuneus. Specifically, the posterior subregion shows connectivity with the lingual and calcarine gyri which are associated with visual processing (Bar et al., 2001; Lalli et al., 2006; Zhang & Li, 2012), while the anterior subregion exhibits greater functional connectivity with the superior parietal cortices and angular gyri which are known to be involved in numerical processing and calculation (Dehaene et al., 2003). These findings support our observation that the posterior precuneus shows blink-related activation in both PF and MA tasks, while the anterior precuneus is preferentially allocated for calculation processing during MA.

### 4.3 | Caveats

As this was the first investigation of cognitive modulation of BROs, some limitations should be noted. First, source localization utilized a distributed source modeling approach which had the advantage of requiring few prior assumptions about source characteristics, but also inherently biases toward sources closer to the cortical surface (Hauk, 2004). Further studies are needed to validate the source space results using alternate approaches such as spatial filtering with beamformer (Hillebrand, Singh, Holliday, Furlong, & Barnes, 2005). Second, although this study provided the initial demonstration of blink-related activation of cortical regions consistent with the VAN, the role of the ventral attention *network* can only be ascertained through network analysis. Given the focus on main effects in this study, a detailed exploration of network relationships was beyond the scope of this study. Further studies are needed to examine the network relationships in more detail. Similarly, additional analyses should also explore the connectivity and causality relationships within the network regions engaged in blink-related processing to validate the hypothesized neurocognitive mechanism for blink processing proposed in this study. Furthermore, as no recordings of mandibular activity were made to ensure that subjects did not verbalize numbers during the MA task, we could not be certain that no such verbalizations took place. Nonetheless, the study did utilize continuous video monitoring of the participants throughout the recording sessions, which helped to monitor general participant behavior during the scans. Additionally, the extensive data preparation and artifact rejection procedures undertaken prior to BRO response derivation helped ensure that any

contamination of the data due to muscular and other physiological sources was kept to a minimum.

## 5 | CONCLUSIONS

This MEG study was the first investigation of blink-related oscillations under cognitive task conditions. We confirmed the presence of BRO effects during both MA and PF tasks by demonstrating the blink-related activation of the bilateral precuneus regions, with concomitant increase in GFP amplitude consistent with previous reports. Moreover, we also demonstrated for the first time that cognitive loading via mental arithmetic modulated BRO effects by decreasing the blink-related activation of key brain regions including the bilateral anterior precuneus and the parahippocampal, lingual, and fusiform gyri—while also activating VAN regions not engaged during PF. Based on an observed pattern of precuneal spectral activity consistent across both tasks, we further postulate a potential neurocognitive mechanism for blink processing in the precuneus. Our findings in this study thus confirm and extend previous reports of BRO effects, and provide compelling new evidence for the important cognitive implications of the BRO phenomenon.

### ACKNOWLEDGMENTS

The authors would like to thank the Down Syndrome Research Foundation for use of their MEG imaging system for data collection. The authors also thank M.C. Graham and Q. Gao for administrative and technical support, and S. Fickling and M. Courtemanche for their assistance with data collection.

### ORCID

Careesa C. Liu  <https://orcid.org/0000-0002-5481-9535>

### REFERENCES

- Aguirre, G. K., Detre, J. A., Alsop, D. C., & D'Esposito, M. (1996). The parahippocampus subserves topographical learning in man. *Cerebral Cortex* (New York, N.Y.: 1991), 6(6), 823–829.
- Aminoff, E. M., Kveraga, K., & Bar, M. (2013). The role of the parahippocampal cortex in cognition. *Trends in Cognitive Sciences*, 17(8), 379–390. <https://doi.org/10.1016/j.tics.2013.06.009>
- Bar, M., Aminoff, E., & Schacter, D. L. (2008). Scenes unseen: The parahippocampal cortex intrinsically subserves contextual associations, not scenes or places per se. *The Journal of Neuroscience: the Official Journal*

- of the Society for Neuroscience, 28(34), 8539–8544. <https://doi.org/10.1523/JNEUROSCI.0987-08.2008>
- Bar, M., Tootell, R. B., Schacter, D. L., Greve, D. N., Fischl, B., Mendola, J. D., ... Dale, A. M. (2001). Cortical mechanisms specific to explicit visual object recognition. *Neuron*, 29(2), 529–535.
- Beauchamp, G. (2015). Chapter 1 - overview of animal vigilance. In G. Beauchamp (Ed.), *Animal Vigilance* (pp. 1–21). San Diego: Academic Press. <https://doi.org/10.1016/B978-0-12-801983-2.00001-2>
- Bentivoglio, A. R., Bressman, S. B., Cassetta, E., Carretta, D., Tonali, P., & Albanese, A. (1997). Analysis of blink rate patterns in normal subjects. *Movement Disorders*, 12(6), 1028–1034. <https://doi.org/10.1002/mds.870120629>
- Berman, B. D., Horowitz, S. G., Morel, B., & Hallett, M. (2012). Neural correlates of blink suppression and the buildup of a natural bodily urge. *NeuroImage*, 59(2), 1441–1450. <https://doi.org/10.1016/j.neuroimage.2011.08.050>
- Bonfiglio, L., Olcese, U., Rossi, B., Frisoli, A., Arrighi, P., Greco, G., ... Carboncini, M. C. (2013). Cortical source of blink-related delta oscillations and their correlation with levels of consciousness. *Human Brain Mapping*, 34(9), 2178–2189. <https://doi.org/10.1002/hbm.22056>
- Bonfiglio, L., Piarulli, A., Olcese, U., Andre, P., Arrighi, P., Frisoli, A., ... Carboncini, M. C. (2014). Spectral parameters modulation and source localization of blink-related alpha and low-beta oscillations differentiate minimally conscious state from vegetative state/unresponsive wakefulness syndrome. *PLoS One*, 9(3), e93252. [10.1371/journal.pone.0093252](https://doi.org/10.1371/journal.pone.0093252)
- Bonfiglio, L., Sello, S., Andre, P., Carboncini, M. C., Arrighi, P., & Rossi, B. (2009). Blink-related delta oscillations in the resting-state EEG: A wavelet analysis. *Neuroscience Letters*, 449(1), 57–60. <https://doi.org/10.1016/j.neulet.2008.10.039>
- Bonfiglio, L., Sello, S., Carboncini, M. C., Arrighi, P., Andre, P., & Rossi, B. (2011). Reciprocal dynamics of EEG alpha and delta oscillations during spontaneous blinking at rest: A survey on a default mode-based visuo-spatial awareness. *International Journal of Psychophysiology*, 80(1), 44–53. <https://doi.org/10.1016/j.ijpsycho.2011.01.002>
- Buckner, R. L., Andrews-Hanna, J. R., & Schacter, D. L. (2008). The brain's default network - anatomy, function, and relevance to disease. *Annals of the New York Academy of Sciences*, 1124, 1–38. <https://doi.org/10.1196/annals.1440.011>
- Buzsáki, G. (2002). Theta oscillations in the hippocampus. *Neuron*, 33(3), 325–340. [https://doi.org/10.1016/S0896-6273\(02\)00586-X](https://doi.org/10.1016/S0896-6273(02)00586-X)
- Cavanna, A. E., & Trimble, M. R. (2006). The precuneus: A review of its functional anatomy and behavioural correlates. *Brain: A Journal of Neurology*, 129(Pt 3), 564–583.
- Chai, W. J., Abd Hamid, A. I., & Abdullah, J. M. (2018). Working memory from the psychological and neurosciences perspectives: A review. *Frontiers in Psychology*, 9(401). <https://doi.org/10.3389/fpsyg.2018.00401>
- Corbetta, M., & Shulman, G. L. (2002). Control of goal-directed and stimulus-driven attention in the brain. *Nature Reviews Neuroscience*, 3(3), 201–215. Retrieved from <https://doi.org/10.1038/nrn755>
- Cunningham, S. I., Tomasi, D., & Volkow, N. D. (2017). Structural and functional connectivity of the precuneus and thalamus to the default mode network. *Human Brain Mapping*, 38(2), 938–956. <https://doi.org/10.1002/hbm.23429>
- Davachi, L., Mitchell, J. P., & Wagner, A. D. (2003). Multiple routes to memory: Distinct medial temporal lobe processes build item and source memories. *Proceedings of the National Academy of Sciences of the United States of America*, 100(4), 2157–2162. <https://doi.org/10.1073/pnas.0337195100>
- Dehaene, S., & Cohen, L. (1995). Towards an anatomical and functional model of number processing. *Mathematical Cognition*, 1(1), 83–120.
- Dehaene, S., Molko, N., Cohen, L., & Wilson, A. J. (2004). Arithmetic and the brain. *Current Opinion in Neurobiology*, 14(2), 218–224. <https://doi.org/10.1016/j.conb.2004.03.008>
- Dehaene, S., Piazza, M., Pinel, P., & Cohen, L. (2003). Three parietal circuits for number processing. *Cognitive Neuropsychology*, 20(3), 487–506. <https://doi.org/10.1080/02643290244000239>
- Delorme, A., & Makeig, S. (2004). EEGLAB: An open source toolbox for analysis of single-trial EEG dynamics including independent component analysis. *Journal of Neuroscience Methods*, 134(1), 9–21. <https://doi.org/10.1016/j.jneumeth.2003.10.009>
- Dickerson, B. C., & Eichenbaum, H. (2010). The episodic memory system: Neurocircuitry and disorders. *Neuropsychopharmacology*, 35(1), 86–104. <https://doi.org/10.1038/npp.2009.126>
- Duzel, E., Habib, R., Rotte, M., Guderian, S., Tulving, E., Heinze, H.-J. J., ... Heinze, H.-J. J. (2003). Human hippocampal and parahippocampal activity during visual associative recognition memory for spatial and nonspatial stimulus configurations. *The Journal of Neuroscience: the Official Journal of the Society for Neuroscience*, 23(28), 9439–9444.
- Epstein, R., & Kanwisher, N. (1998). A cortical representation of the local visual environment. *Nature*, 392(6676), 598–601. <https://doi.org/10.1038/33402>
- Epstein, R. A., & Ward, E. J. (2010). How reliable are visual context effects in the parahippocampal place area? *Cerebral Cortex (New York, N.Y.: 1991)*, 20(2), 294–303. <https://doi.org/10.1093/cercor/bhp099>
- Fehr, T., Code, C., & Herrmann, M. (2007). Common brain regions underlying different arithmetic operations as revealed by conjunct fMRI-BOLD activation. *Brain Research*, 1172, 93–102. <https://doi.org/10.1016/j.brainres.2007.07.043>
- Fitzgibbon, S. P., Pope, K. J., Mackenzie, L., Clark, C. R., & Willoughby, J. O. (2004). Cognitive tasks augment gamma EEG power. *Clinical Neurophysiology*, 115(8), 1802–1809. <https://doi.org/10.1016/j.clinph.2004.03.009>
- Foxe, J. J., Simpson, G. V., & Ahlfors, S. P. (1998). Parieto-occipital approximately 10 Hz activity reflects anticipatory state of visual attention mechanisms. *Neuroreport*, 9(17), 3929–3933.
- Friston, K. J., Holmes, A. P., Worsley, K. J., Poline, J.-P., Frith, C. D., & Frackowiak, R. S. J. (1994). Statistical parametric maps in functional imaging: A general linear approach. *Human Brain Mapping*, 2(4), 189–210. <https://doi.org/10.1002/hbm.460020402>
- Ghosh Hajra, S., Liu, C. C., Song, X., Fickling, S., Liu, L., Pawlowski, G., ... D'Arcy, R. (2016). Developing brain vital signs: Initial framework for monitoring brain function changes over time. *Frontiers in Neuroscience*, 10, 211. <https://doi.org/10.3389/fnins.2016.00211>
- Ghosh Hajra, S., Liu, C. C., Song, X., Fickling, S. D., Cheung, T. P. L., & D'Arcy, R. C. N. (2018). Multimodal characterization of the semantic N400 response within a rapid evaluation brain vital sign framework. *Journal of Translational Medicine*, 16(1), 151. <https://doi.org/10.1186/s12967-018-1527-2>
- Grabner, R. H., Ansari, D., Koschutnig, K., Reishofer, G., Ebner, F., & Neuper, C. (2009). To retrieve or to calculate? Left angular gyrus mediates the retrieval of arithmetic facts during problem solving. *Neuropsychologia*, 47(2), 604–608. <https://doi.org/10.1016/j.neuropsychologia.2008.10.013>
- Greenberg, J. A., Burke, J. F., Haque, R., Kahana, M. J., & Zaghlool, K. A. (2015). Decreases in theta and increases in high frequency activity underlie associative memory encoding. *NeuroImage*, 114, 257–263. <https://doi.org/10.1016/j.neuroimage.2015.03.077>
- Gusnard, D. A., & Raichle, M. E. (2001). Searching for a baseline: Functional imaging and the resting human brain. *Nature Reviews Neuroscience*, 2(10), 685–694. <https://doi.org/10.1038/35094500>
- Hagemann, D., Naumann, E., & Thayer, J. F. (2001). The quest for the EEG reference revisited: A glance from brain asymmetry research. *Psychophysiology*, 38(5), 847–857.
- Hagmann, P., Cammoun, L., Gigandet, X., Meuli, R., Honey, C. J., Wedeen, V. J., & Sporns, O. (2008). Mapping the structural core of human cerebral cortex. *PLoS Biology*, 6(7), 1479–1493. <https://doi.org/10.1371/journal.pbio.0060159>
- Hauk, O. (2004). Keep it simple: A case for using classical minimum norm estimation in the analysis of EEG and MEG data. *NeuroImage*, 21(4), 1612–1621. <https://doi.org/10.1016/j.neuroimage.2003.12.018>
- He, B. J., & Raichle, M. E. (2009). The fMRI signal, slow cortical potential and consciousness. *Trends in Cognitive Sciences*, 13(7), 302–309. <https://doi.org/10.1016/J.TICS.2009.04.004>
- Hebart, M. N., & Hesselmann, G. (2012). What visual information is processed in the human dorsal stream? *The Journal of Neuroscience*, 32(24), 8107.
- Hillebrand, A., Singh, K. D., Holliday, I. E., Furlong, P. L., & Barnes, G. R. (2005). A new approach to neuroimaging with magnetoencephalography.

- Human Brain Mapping*, 25(2), 199–211. <https://doi.org/10.1002/hbm.20102>
- Ischebeck, A., Zamarian, L., Siedentopf, C., Koppelstätter, F., Benke, T., Felber, S., & Delazer, M. (2006). How specifically do we learn? Imaging the learning of multiplication and subtraction. *NeuroImage*, 30(4), 1365–1375.
- Ishii, R., Canuet, L., Ishihara, T., Aoki, Y., Ikeda, S., Hata, M., ... Takeda, M. (2014). Frontal midline theta rhythm and gamma power changes during focused attention on mental calculation: An MEG beamformer analysis. *Frontiers in Human Neuroscience*, 8, 406.
- Jensen, O., & Mazaheri, A. (2010). Shaping functional architecture by oscillatory alpha activity: Gating by inhibition. *Frontiers in Human Neuroscience*, 4, 186. <https://doi.org/10.3389/fnhum.2010.00186>
- Kelly, S. P., Lalor, E. C., Reilly, R. B., & Foxe, J. J. (2006). Increases in alpha oscillatory power reflect an active retinotopic mechanism for distracter suppression during sustained visuospatial attention. *Journal of Neurophysiology*, 95(6), 3844–3851.
- Kirwan, C. B., & Stark, C. E. (2004). Medial temporal lobe activation during encoding and retrieval of novel face-name pairs. *Hippocampus*, 14(7), 919–930. <https://doi.org/10.1002/hipo.20014>
- Klein, E., Moeller, K., Glauche, V., Weiller, C., & Willmes, K. (2013). Processing pathways in mental Arithmetic: Evidence from probabilistic fiber tracking. *PLoS One*, 8(1), e55455.
- Klimesch, W. (2012). Alpha-band oscillations, attention, and controlled access to stored information. *Trends in Cognitive Sciences*, 16(12), 606–617.
- Klimesch, W., Sauseng, P., & Hanslmayr, S. (2007). EEG alpha oscillations: The inhibition–timing hypothesis. *Brain Research Reviews*, 53(1), 63–88. <https://doi.org/10.1016/j.brainresrev.2006.06.003>
- Kong, J., Wang, C., Kwong, K., Vangel, M., Chua, E., & Gollub, R. (2005). The neural substrate of arithmetic operations and procedure complexity. *Cognitive Brain Research*, 22(3), 397–405. <https://doi.org/10.1016/j.cogbrainres.2004.09.011>
- Lalli, S., Hussain, Z., Ayub, A., Cracco, R. Q., Bodis-Wollner, I., & Amassian, V. E. (2006). Role of the calcarine cortex (V1) in perception of visual cues for saccades. *Clinical Neurophysiology*, 117(9), 2030–2038. <https://doi.org/10.1016/j.clinph.2006.05.022>
- Litvak, V., & Friston, K. (2008). Electromagnetic source reconstruction for group studies. *NeuroImage*, 42(4), 1490–1498. <https://doi.org/10.1016/j.neuroimage.2008.06.022>
- Litvak, V., Mattout, Z., Kiebel, S., Phillips, C., Henson, R., Kilner, J., ... Friston, K. (2011). EEG and MEG data analysis in SPM8. *Computational Intelligence and Neuroscience*, 2011, 852961, 1–852932. <https://doi.org/10.1155/2011/852961>
- Liu, C. C., Ghosh Hajra, S., Cheung, T. P. L., Song, X., & D'Arcy, R. C. N. (2017). Spontaneous blinks activate the precuneus: Characterizing blink-related oscillations using magnetoencephalography. *Frontiers in Human Neuroscience*, 11, 489. <https://doi.org/10.3389/fnhum.2017.00489>
- Luking, K. R., Nelson, B. D., Infantolino, Z. P., Sauder, C. L., & Hajcak, G. (2017). Internal consistency of functional magnetic resonance imaging and electroencephalography measures of reward in late childhood and early adolescence. *Biological Psychiatry: Cognitive Neuroscience and Neuroimaging*, 2(3), 289–297. <https://doi.org/10.1016/j.bpsc.2016.12.004>
- Machielsen, W. C., Rombouts, S. A., Barkhof, F., Scheltens, P., & Witter, M. P. (2000). fMRI of visual encoding: Reproducibility of activation. *Human Brain Mapping*, 9(3), 156–164.
- Makeig, S. (1993). Auditory event-related dynamics of the EEG spectrum and effects of exposure to tones. *Electroencephalography and Clinical Neurophysiology*, 86(4), 283–293.
- Makeig, S., Bell, A. J., Jung, T.-P., & Sejnowski, T. J. (1996). Independent component analysis of electroencephalographic data. In D. Touretzky, M. Mozer, & M. Hasselmo (Eds.), *Advances in neural information processing systems* (Vol. 8, pp. 145–151). Cambridge, MA: The MIT Press.
- Manning, K. A., Riggs, L. A., & Komenda, J. K. (1983). Reflex eyeblinks and visual suppression. *Perception & Psychophysics*, 34(3), 250–256.
- Marinova, I., & Mateev, V. (2010). Electromagnetic field modeling in human tissue. *International Journal of Medical, Health, Biomedical, Bioengineering and Pharmaceutical Engineering*, 4, 140–145.
- Matsumoto, J. Y., Stead, M., Kucewicz, M. T., Matsumoto, A. J., Peters, P. A., Brinkmann, B. H., ... Worrell, G. A. (2013). Network oscillations modulate interictal epileptiform spike rate during human memory. *Brain: A Journal of Neurology*, 136(Pt 8), 2444–2456. <https://doi.org/10.1093/brain/awt159>
- Matsumoto-Oda, A., Okamoto, K., Takahashi, K., & Ohira, H. (2018). Group size effects on inter-blink interval as an indicator of antipredator vigilance in wild baboons. *Scientific Reports*, 8(1), 10062. <https://doi.org/10.1038/s41598-018-28174-7>
- Mellet, E., Bricogne, S., Tzourio-Mazoyer, N., Ghaem, O., Petit, L., Zago, L., ... Denis, M. (2000). Neural correlates of topographic mental exploration: The impact of route versus survey perspective learning. *NeuroImage*, 12, 588–600. <https://doi.org/10.1006/nimg.2000.0648>
- Menon, V. (2010). Developmental cognitive neuroscience of arithmetic: Implications for learning and education. *ZDM*, 42(6), 515–525. <https://doi.org/10.1007/s11858-010-0242-0>
- Mitchell, D. J., & Cusack, R. (2011). The temporal evolution of electromagnetic markers sensitive to the capacity limits of visual short-term memory. *Frontiers in Human Neuroscience*, 5, 18. <https://doi.org/10.3389/fnhum.2011.00018>
- Nakano, T. (2015). Blink-related dynamic switching between internal and external orienting networks while viewing videos. *Neuroscience Research*, 96, 54–58. <https://doi.org/10.1016/j.neures.2015.02.010>
- Nakano, T., Kato, M., Morito, Y., Itoi, S., & Kitazawa, S. (2013). Blink-related momentary activation of the default mode network while viewing videos. *Proceedings of the National Academy of Sciences of the United States of America*, 110(2), 702–706. <https://doi.org/10.1073/pnas.1214804110>
- Nunez, P. L., Silberstein, R. B., Cadusch, P. J., Wijesinghe, R. S., Westdorp, A. F., & Srinivasan, R. (1994). A theoretical and experimental study of high resolution EEG based on surface Laplacians and cortical imaging. *Electroencephalography and Clinical Neurophysiology*, 90(1), 40–57. [https://doi.org/10.1016/0013-4694\(94\)90112-0](https://doi.org/10.1016/0013-4694(94)90112-0)
- Oh, J., Han, M., Peterson, B. S., & Jeong, J. (2012). Spontaneous eyeblinks are correlated with responses during the Stroop task. *PLoS One*, 7(4), e34871–e34871. <https://doi.org/10.1371/journal.pone.0034871>
- Park, S., & Chun, M. M. (2009). Different roles of the parahippocampal place area (PPA) and retrosplenial cortex (RSC) in panoramic scene perception. *NeuroImage*, 47(4), 1747–1756. <https://doi.org/10.1016/j.neuroimage.2009.04.058>
- Perry, G., Hamandi, K., Brindley, L. M., Muthukumaraswamy, S. D., & Singh, K. D. (2013). The properties of induced gamma oscillations in human visual cortex show individual variability in their dependence on stimulus size. *NeuroImage*, 68, 83–92. <https://doi.org/10.1016/j.neuroimage.2012.11.043>
- Pfefferbaum, A., Chanraud, S., Pitel, A.-L., Muller-Oehring, E., Shankaranarayanan, A., Alsop, D. C., ... Sullivan, E. V. (2011). Cerebral blood flow in posterior cortical nodes of the default mode network decreases with task engagement but remains higher than in most brain regions. *Cerebral Cortex*, 21(1), 233–244. <https://doi.org/10.1093/cercor/bhq090>
- Raichle, M. E., MacLeod, A. M., Snyder, A. Z., Powers, W. J., Gusnard, D. A., & Shulman, G. L. (2001). A default mode of brain function. *Proceedings of the National Academy of Sciences of the United States of America*, 98(2), 676–682. <https://doi.org/10.1073/pnas.98.2.676>
- Raz, S., Bar-Haim, Y., Sadeh, A., & Dan, O. (2014). Reliability and validity of the online continuous performance test among young adults. *Assessment*, 21(1), 108–118. <https://doi.org/10.1177/1073191112443409>
- Riggs, L. A., Volkman, F. C., & Moore, R. K. (1981). Suppression of the blackout due to blinks. *Vision Research*, 21(7), 1075–1079. [https://doi.org/10.1016/0042-6989\(81\)90012-2](https://doi.org/10.1016/0042-6989(81)90012-2)
- Sauseng, P., Klimesch, W., Heise, K. F., Gruber, W. R., Holz, E., Karim, A. A., ... Hummel, F. C. (2009). Brain oscillatory substrates of visual short-term memory capacity. *Current Biology: CB*, 19(21), 1846–1852. <https://doi.org/10.1016/j.cub.2009.08.062>
- Schadow, J., Lenz, D., Thaeerig, S., Busch, N. A., Fründ, I., Rieger, J. W., & Herrmann, C. S. (2007). Stimulus intensity affects early sensory processing: Visual contrast modulates evoked gamma-band activity in human EEG. *International Journal of Psychophysiology*, 66, 28–36. <https://doi.org/10.1016/j.ijpsycho.2007.05.010>
- Siegle, G. J., Ichikawa, N., & Steinhauer, S. (2008). Blink before and after you think: Blinks occur prior to and following cognitive load indexed



- by pupillary responses. *Psychophysiology*, 45(5), 679–687. <https://doi.org/10.1111/j.1469-8986.2008.00681.x>
- Skrandies, W. (1990). Global field power and topographic similarity. *Brain Topography*, 3(1), 137–141. <https://doi.org/10.1007/BF01128870>
- Tan, H. R. M., Lana, L., & Uhlhaas, P. J. (2013). High-frequency neural oscillations and visual processing deficits in schizophrenia. *Frontiers in Psychology*, 4, 10. <https://doi.org/10.3389/fpsyg.2013.00621>
- Thut, G., Nietzel, A., Brandt, S. A., & Pascual-Leone, A. (2006). Alpha-band electroencephalographic activity over occipital cortex indexes visuo-spatial attention bias and predicts visual target detection. *The Journal of Neuroscience : the Official Journal of the Society for Neuroscience*, 26(37), 9494–9502.
- Tsubota, K., Kwong, K. K., Lee, T. Y., Nakamura, J., & Cheng, H. M. (1999). Functional MRI of brain activation by eye blinking. *Experimental Eye Research*, 69(1), 1–7. <https://doi.org/10.1006/exer.1999.0660>
- Wascher, E., Heppner, H., Möckel, T., Kobald, S. O., & Getzmann, S. (2015). Eye-blinks in choice response tasks uncover hidden aspects of information processing. *EXCLI Journal*, 14, 1207–1218. <https://doi.org/10.17179/excli2015-696>
- Weiner, K. S., & Zilles, K. (2016). The anatomical and functional specialization of the fusiform gyrus. *Special issue: Functional selectivity in perceptual and cognitive systems - a tribute to Shlomo Bentin (1946–2012)*, 83, 48–62. <https://doi.org/10.1016/j.neuropsychologia.2015.06.033>
- Zarnhofer, S., Braunstein, V., Ebner, F., Koschutnig, K., Neuper, C., Ninaus, M., ... Ischebeck, A. (2013). Individual differences in solving arithmetic word problems. *Behavioral and Brain Functions*, 9, 28.
- Zarnhofer, S., Braunstein, V., Ebner, F., Koschutnig, K., Neuper, C., Reishofer, G., & Ischebeck, A. (2012). The influence of verbalization on the pattern of cortical activation during mental arithmetic. *Behavioral and Brain Functions*, 8, 13. <https://doi.org/10.1186/1744-9081-8-13>
- Zhang, H., & Jacobs, J. (2015). Traveling theta waves in the human hippocampus. *The Journal of Neuroscience*, 35(36), 12477–12487. <https://doi.org/10.1523/JNEUROSCI.5102-14.2015>
- Zhang, S., & Li, C. S. (2012). Functional connectivity mapping of the human precuneus by resting state fMRI. *NeuroImage*, 59(4), 3548–3562. <https://doi.org/10.1016/j.neuroimage.2011.11.023>

## SUPPORTING INFORMATION

Additional supporting information may be found online in the Supporting Information section at the end of the article.

**How to cite this article:** Liu CC, Hajra SG, Song X, Doesburg SM, Cheung TPL, D'Arcy RCN. Cognitive loading via mental arithmetic modulates effects of blink-related oscillations on precuneus and ventral attention network regions. *Hum Brain Mapp*. 2019;40:377–393. <https://doi.org/10.1002/hbm.24378>